

Synthesis, Structures, and Magnetic Properties of Heterodimetal Bis(μ -hydroxo)chromium(III)nickel(II) Complexes with Tpa Derivatives Having Sterically Bulky Substituents

Kazushi Shiren, Shuhei Fujinami, Masatatsu Suzuki,* and Akira Uehara*

Department of Chemistry, Faculty of Science, Kanazawa University, Kakuma-machi, Kanazawa 920-1192, Japan

Received May 29, 2001

A series of heterodinuclear bis(μ -hydroxo)chromium(III)nickel(II) complexes was newly prepared: [(phen)₂Cr(μ -OH)₂Ni(tpa)](ClO₄)₃·0.5H₂O (**1**), [(phen)₂Cr(μ -OH)₂Ni(Me-tpa)](ClO₄)₃·2H₂O (**2**), [(phen)₂Cr(μ -OH)₂Ni(Me₂-tpa)](ClO₄)₃·2H₂O (**3**), and [(phen)₂Cr(μ -OH)₂Ni(Me₃-tpa)](ClO₄)₃·3H₂O (**4**), where phen is 1,10-phenanthroline and tpa, Me-tpa, Me₂-tpa, and Me₃-tpa are tris(2-pyridylmethyl)amine, [(6-methyl-2-pyridyl)methyl]bis(2-pyridylmethyl)amine, bis[(6-methyl-2-pyridyl)methyl](2-pyridylmethyl)amine, and tris[(6-methyl-2-pyridyl)methyl]amine, respectively. X-ray crystallography revealed that the structures of **1–4** resemble one another having an edge-shared bioctahedral structure with a Cr(μ -OH)₂Ni unit (crystal data: **1**·C₂H₅OH, triclinic, $P\bar{1}$, $a = 13.179(4)$ Å, $b = 13.685(4)$ Å, $c = 14.260(4)$ Å, $\alpha = 84.95(2)^\circ$, $\beta = 77.65(1)^\circ$, $\gamma = 90.21(2)^\circ$, $V = 2502(1)$ Å³, $Z = 2$, $R = 0.103$, $R_w = 0.097$; **2**·C₂H₅OH, triclinic, $P\bar{1}$, $a = 13.214(2)$ Å, $b = 13.657(2)$ Å, $c = 14.417(3)$ Å, $\alpha = 95.205(5)^\circ$, $\beta = 102.583(4)^\circ$, $\gamma = 90.720(3)^\circ$, $V = 2527.3(8)$ Å³, $Z = 2$, $R = 0.090$, $R_w = 0.122$; **3**·C₂H₅OH, triclinic, $P\bar{1}$, $a = 13.276(2)$ Å, $b = 13.696(2)$ Å, $c = 14.454(2)$ Å, $\alpha = 95.640(3)^\circ$, $\beta = 102.821(4)^\circ$, $\gamma = 90.174(3)^\circ$, $V = 2549.5(6)$ Å³, $Z = 2$, $R = 0.087$, $R_w = 0.119$; **4**, triclinic, $P\bar{1}$, $a = 10.8916(9)$ Å, $b = 14.268(2)$ Å, $c = 17.522(2)$ Å, $\alpha = 84.498(9)^\circ$, $\beta = 74.313(7)^\circ$, $\gamma = 72.402(7)^\circ$, $V = 2498.6(5)$ Å³, $Z = 2$, $R = 0.060$, $R_w = 0.088$). Chromium and nickel ions are coordinated by two phen's and Me_{*n*}-tpa, respectively, to complete a distorted octahedral coordination sphere. Introduction of the 6-methyl group(s) onto the pyridyl group(s) results in the elongation of the Ni–N bond distances due to an unfavorable steric interaction between the methyl group and the bridging hydroxide group: systematic elongation of the Ni–N bond distances and the Cr···Ni separations accompanied by an increase in the Cr–O–Ni angles was observed as the number of the methyl groups increases. Variable-temperature magnetic susceptibility measurements of **1–4** (4.2–300 K) indicated that magnetic interactions between Cr(III) and Ni(II) ions are systematically modulated from a very weak antiferromagnetic interaction to a ferromagnetic interaction as the number of the methyl groups increases; the exchange integrals J s for **1–4** are estimated to be -1.4 , $+0.0$, $+4.1$, and $+7.4$ cm⁻¹, respectively. The magneto–structural relationship is discussed in terms of the change in the magnetic orbital energies of nickel(II) centers arising from the change in the Ni–N bond distances.

Introduction

A variety of heterobimetallic complexes containing chromium(III) and nickel(II) ions have been developed for constructing complex-based ferromagnetic materials. Compounds containing oxalate,^{1–3} dithiooxalate,⁴ or cyanide^{5–8} as the bridging group exhibit ferromagnetic interaction

between chromium(III) and nickel(II) ions with the exchange integrals J in the range $+2.7$ to $+8.4$ cm⁻¹ based on the

* Corresponding author. Tel: +81-76-264-5701 (M.S.). Fax: +81-76-264-5742 (M.S.). E-mail: suzuki@cacheibm.s.kanazawa-u.ac.jp (M.S.); uehara@cacheibm.s.kanazawa-u.ac.jp (A.U.).

(1) Pei, Y.; Journaux, Y.; Kahn, O. *Inorg. Chem.* **1989**, *28*, 100–103.

(2) Tamaki, H.; Zhong, Z. J.; Matsumoto, N.; Kida, S.; Koikawa, M.; Achiwa, N.; Hashimoto, Y.; Okawa, H. *J. Am. Chem. Soc.* **1992**, *114*, 6974–6979.

(3) Ohba, M.; Tamaki, H.; Matsumoto, N.; Okawa, H. *Inorg. Chem.* **1993**, *32*, 5385–5390.

(4) (a) Mitsumi, M.; Okawa, H.; Sakiyama, H.; Ohba, M.; Matsumoto, N.; Kurisaki, T.; Wakita, H. *J. Chem. Soc., Dalton Trans.* **1993**, 2991–2994. (b) Okawa, H.; Mitsumi, M.; Ohba, M.; Koderu, M.; Matsumoto, N. *Bull. Chem. Soc. Jpn.* **1994**, *67*, 2139–2144.

(5) Gadet, V.; Mallah, T.; Castro, I.; Verdaguier, M. *J. Am. Chem. Soc.* **1992**, *114*, 9213–9214.

spin Hamiltonian $H = -2JS_1S_2$. In these systems, the ferromagnetic interaction has been shown to be due to the orthogonality of the magnetic orbitals. In contrast, there are only a few complexes having bridging hydroxide(s). A tetranuclear complex with $\text{Cr}^{\text{III}}(\mu\text{-OH})_2\text{Ni}^{\text{II}}$ units, $[\text{Ni}\{(\text{OH})_2\text{-Cr}(\text{bispictn})\}_3](\text{ClO}_4)_3 \cdot 6\text{H}_2\text{O}$,⁹ and a trinuclear complex with $\text{Cr}^{\text{III}}(\mu\text{-OH})\text{Ni}^{\text{II}}$ units, $[\text{Ni}(\text{H}_2\text{O})_4\{(\text{OH})\text{Cr}(\text{pico})_2(\text{OH})_2\}_2](\text{S}_2\text{O}_6)_2 \cdot \text{H}_2\text{O}$,¹⁰ have been reported, although their structures have not been determined. In contrast to the compounds having an oxalate, dithiooxalate, or cyanide bridge, the hydroxide-bridged complexes exhibit very weak antiferromagnetic interactions between chromium(III) and nickel(II) ions with J values -2.4 and -4.2 cm^{-1} . Thus it is interesting to develop heterodimetal chromium(III)–nickel(II) complexes with hydroxo bridge(s) and investigate their magneto–structural relationship.

In this study, we synthesized a series of new heterodimetal chromium(III)–nickel(II) complexes with a $\text{Cr}^{\text{III}}(\mu\text{-OH})_2\text{Ni}^{\text{II}}$ unit, $[(\text{phen})_2\text{Cr}(\mu\text{-OH})_2\text{Ni}(\text{tpa})](\text{ClO}_4)_3 \cdot 0.5\text{H}_2\text{O}$ (**1**), $[(\text{phen})_2\text{Cr}(\mu\text{-OH})_2\text{Ni}(\text{Me-tpa})](\text{ClO}_4)_3 \cdot 2\text{H}_2\text{O}$ (**2**), $[(\text{phen})_2\text{Cr}(\mu\text{-OH})_2\text{Ni}(\text{Me}_2\text{-tpa})](\text{ClO}_4)_3 \cdot 2\text{H}_2\text{O}$ (**3**), and $[(\text{phen})_2\text{Cr}(\mu\text{-OH})_2\text{Ni}(\text{Me}_3\text{-tpa})](\text{ClO}_4)_3 \cdot 3\text{H}_2\text{O}$ (**4**),¹¹ to investigate the factors which affect the magnetic interactions between chromium(III) and nickel(II) ions through bridging hydroxides by changing the stereochemistry and the electronic properties of the nickel centers by successive introduction of the 6-methyl group onto the pyridyl groups of the tripodal tetradentate ligand, tpa. It has been shown that the introduction of the 6-methyl group onto the pyridyl group tends to elongate the M–N(pyridyl) bond distance due to an unfavorable steric interaction, which leads to weakening of the electron donor ability of the pyridyl group.^{12–15} It is interesting to investigate how such stereochemical and electronic changes affect the magnetic inter-

action between chromium(III) and nickel(II) ions. Herein we report the syntheses, structures, and magneto–structural relationship of a series of $[(\text{phen})_2\text{Cr}(\mu\text{-OH})_2\text{Ni}(\text{Me}_n\text{-tpa})]^{3+}$ complexes in which magnetic interactions between chromium(III) and nickel(II) ions are systematically modulated by successive introduction of the 6-methyl group onto the pyridyl group.

Experimental Section

Materials. Acetonitrile was purified by distillation over calcium hydride. 2-Pyridinecarbaldehyde and 6-methylpyridine-2-carbaldehyde were purified by distillation under reduced pressure. All other reagents and solvents were commercially available and used without further purification.

Preparation of Ligands. Tris(2-pyridylmethyl)amine (tpa). This was prepared according to the literature.¹⁶

[(6-Methyl-2-pyridyl)methyl]bis(2-pyridylmethyl)amine (Me-tpa), Bis[(6-methyl-2-pyridyl)methyl](2-pyridylmethyl)amine (Me₂-tpa), and Tris[(6-methyl-2-pyridyl)methyl]amine (Me₃-tpa). These were prepared as described previously.¹⁷

Preparation of Complexes. $[\text{Cr}(\text{OH})_2(\text{phen})_2](\text{NO}_3)_3 \cdot 2\text{H}_2\text{O}$. This was obtained according to the literature.¹⁸

(Caution: All the perchlorate salts are potentially explosive and should be handled with care!)

$[(\text{phen})_2\text{Cr}(\mu\text{-OH})_2\text{Ni}(\text{tpa})](\text{ClO}_4)_3 \cdot 0.5\text{H}_2\text{O}$ (1**).** To a solution of $[\text{Cr}(\text{OH})_2(\text{phen})_2](\text{NO}_3)_3 \cdot 2\text{H}_2\text{O}$ (335 mg, 0.50 mmol) in methanol (5.0 cm³) was added 2 M aqueous sodium hydroxide (0.50 cm³, 1.00 mmol) at 60 °C to give a brown solution. To this solution, a mixture of tpa (145 mg, 0.50 mmol) and $\text{Ni}(\text{ClO}_4)_2 \cdot 6\text{H}_2\text{O}$ (183 mg, 0.50 mmol) in methanol (1.0 cm³) was added, and the resulting solution was warmed to 60 °C. After addition of NaClO_4 (5 mol dm⁻³, 2.0 cm³), the solution was cooled to ambient temperature. Green crystalline solids formed were collected by filtration. Yield: 489 mg (88%). Anal. Calcd for $\text{C}_{42}\text{H}_{37}\text{N}_8\text{O}_{14.5}\text{Cl}_3\text{CrNi}$: C, 45.74; H, 3.38; N, 10.16; Cr, 4.71; Ni, 5.32. Found: C, 45.92; H, 3.44; N, 10.35; Cr, 4.7; Ni, 5.4. IR (Nujol, cm⁻¹): 3608 (OH), 1605 (C=C, aromatic), 1095 (ClO_4^-), 623 (ClO_4^-).

$[(\text{phen})_2\text{Cr}(\mu\text{-OH})_2\text{Ni}(\text{Me-tpa})](\text{ClO}_4)_3 \cdot 2\text{H}_2\text{O}$ (2**).** The complex was prepared by the same method as that of **1** except that Me-tpa was used instead of tpa. Yield: 423 mg (74%). Anal. Calcd for $\text{C}_{43}\text{H}_{42}\text{N}_8\text{O}_{16}\text{Cl}_3\text{CrNi}$: C, 45.15; H, 3.70; N, 9.80; Cr, 4.55; Ni, 5.13. Found: C, 45.02; H, 3.49; N, 9.80; Cr, 4.5; Ni, 5.2. IR (Nujol, cm⁻¹): 1605 (C=C, aromatic), 1086 (ClO_4^-), 623 (ClO_4^-).

$[(\text{phen})_2\text{Cr}(\mu\text{-OH})_2\text{Ni}(\text{Me}_2\text{-tpa})](\text{ClO}_4)_3 \cdot 2\text{H}_2\text{O}$ (3**).** This was obtained as green crystals in a manner similar to that of **1** except that Me₂-tpa was used instead of tpa. Yield: 420 mg (73%). Anal. Calcd for $\text{C}_{44}\text{H}_{44}\text{N}_8\text{O}_{16}\text{Cl}_3\text{CrNi}$: C, 45.64; H, 3.83; N, 9.68; Cr, 4.49; Ni, 5.07. Found: C, 45.25; H, 3.80; N, 9.90; Cr, 4.5; Ni, 5.1. IR (Nujol, cm⁻¹): 1606 (C=C, aromatic), 1093 (ClO_4^-), 623 (ClO_4^-).

$[(\text{phen})_2\text{Cr}(\mu\text{-OH})_2\text{Ni}(\text{Me}_3\text{-tpa})](\text{ClO}_4)_3 \cdot 3\text{H}_2\text{O}$ (4**).** The compound was obtained as green crystals by a method similar to that of **1** except that Me₃-tpa was used instead of tpa. Green crystals suitable for X-ray crystallography were obtained. Yield: 430 mg (72%). Anal. Calcd for $\text{C}_{45}\text{H}_{48}\text{N}_8\text{O}_{17}\text{Cl}_3\text{CrNi}$: C, 45.42; H, 4.07; N, 9.42; Cr, 4.37; Ni, 4.93. Found: C, 45.35; H, 4.04; N, 9.32; Cr,

- (6) Mallah, T.; Auberger, C.; Verdagner, M.; Veillet, P. *J. Chem. Soc., Chem. Commun.* **1995**, 61–62.
 (7) (a) Ohkoshi, S.; Sato, O.; Iyoda, T.; Fujishima, A.; Hashimoto, K. *Inorg. Chem.* **1997**, *36*, 268–269. (b) Ohkoshi, S.; Iyoda, T.; Fujishima, A.; Hashimoto, K. *Phys. Rev. B.* **1997**, *56*, 11642–11652.
 (8) Ohba, M.; Okawa, H.; Fukita, N.; Hashimoto, Y. *J. Am. Chem. Soc.* **1997**, *119*, 1011–1019.
 (9) Hodgson, D. J.; Michelsen, K.; Pedersen, E.; Towle, D. K. *Inorg. Chem.* **1991**, *30*, 815–822.
 (10) Corbin, K. M.; Glerup, J.; Hodgson, D. J.; Lynn, M. H.; Michelsen, K.; Nielsen, K. M. *Inorg. Chem.* **1993**, *32*, 18–26.
 (11) Abbreviations of ligands used: tpa = tris(2-pyridylmethyl)amine; Me-tpa = (6-methyl-2-pyridylmethyl)bis(2-pyridylmethyl)amine; Me₂-tpa = bis(6-methyl-2-pyridylmethyl)(2-pyridylmethyl)amine; Me₃-tpa = tris(6-methyl-2-pyridylmethyl)amine; taea = tri(2-aminoethyl)amine; bispictn = *N,N'*-bis(2-pyridylmethyl)-1,3-diaminopropane; pico = 2-pyridylmethylamine; Me₆-[14]ane-N₄ = (±)-5,7,7,12,14,14-hexamethyl-1,4,8,11-tetraazacyclotetradecane; taea = tris(2-aminoethyl)amine; H₂ox = oxalic acid; H₂dto = dithiooxalic acid; tetren = tetraethylenepentamine.
 (12) (a) Goodson, P. A.; Hodgson, D. J. *Inorg. Chem.* **1989**, *28*, 3606–3608. (b) Goodson, P. A.; Oki, A. R.; Glerup, J.; Hodgson, D. J. *J. Am. Chem. Soc.* **1990**, *112*, 6248–6254.
 (13) (a) Zang, Y.; Pan, G.; Que, L., Jr.; Fox, B. G.; Münck, E. *J. Am. Chem. Soc.* **1994**, *116*, 3653–3654. (b) Zang, Y.; Dong, Y.; Que, L., Jr.; Kauffmann, K.; Münck, E. *J. Am. Chem. Soc.* **1995**, *117*, 1169–1170. (c) Zang, Y.; Kim, J.; Dong, Y.; Wilkinson, E. C.; Appelman, E. H.; Que, L., Jr. *J. Am. Chem. Soc.* **1997**, *119*, 4197–4205.
 (14) Hayashi, Y.; Kayatani, T.; Sugimoto, H.; Suzuki, M.; Inomata, K.; Uehara, A.; Mizutani, Y.; Kitagawa, T.; Maeda, Y. *J. Am. Chem. Soc.* **1995**, *117*, 11220–11229.
 (15) Shiren, K.; Ogo, S.; Fujinami, S.; Hayashi, H.; Suzuki, M.; Uehara, A.; Watanabe, Y.; Moro-oka, Y. *J. Am. Chem. Soc.* **2000**, *122*, 254–262.

- (16) Anderegg, G.; F. Wenk, *Helv. Chim. Acta.* **1967**, *50*, 2330–2332.
 (17) Nagao, H.; Komeda, N.; Mukaida, M.; Suzuki, M.; Tanaka, K. *Inorg. Chem.* **1996**, *35*, 6809–6815.
 (18) Hancock, M. P.; Josephsen, J.; Schäffer, C. E. *Acta Chem. Scand.* **1976**, *A30*, 79–97.

Table 1. Crystallographic Data for [(phen)₂Cr(μ -OH)₂Ni(tpa)](ClO₄)₃·C₂H₅OH·0.75H₂O (**1**·C₂H₅OH), [(phen)₂Cr(μ -OH)₂Ni(Me-tpa)](ClO₄)₃·C₂H₅OH·0.75H₂O (**2**·C₂H₅OH), [(phen)₂Cr(μ -OH)₂Ni(Me₂-tpa)](BF₄)₃·C₂H₅OH·H₂O (**3**·C₂H₅OH), and [(phen)₂Cr(μ -OH)₂Ni(Me₃-tpa)](ClO₄)₃·3H₂O (**4**)

	1 ·C ₂ H ₅ OH	2 ·C ₂ H ₅ OH	3 ·C ₂ H ₅ OH	4
formula	C ₄₄ H _{43.5} N ₈ O _{15.75} Cl ₃ CrNi	C ₄₅ H _{45.5} N ₈ O _{15.75} Cl ₃ CrNi	C ₄₆ H ₄₈ N ₈ O ₁₆ Cl ₃ CrNi	C ₄₅ H ₄₈ N ₈ O ₁₇ Cl ₃ CrNi
temp, °C	-150	-150	-150	-150
MW	1153.43	1167.45	1185.98	1189.97
cryst system	triclinic	triclinic	triclinic	triclinic
space group	<i>P</i> $\bar{1}$	<i>P</i> $\bar{1}$	<i>P</i> $\bar{1}$	<i>P</i> $\bar{1}$
<i>a</i> , Å	13.179(4)	13.214(2)	13.276(2)	10.8916(9)
<i>b</i> , Å	13.685(4)	13.657(2)	13.696(2)	14.268(2)
<i>c</i> , Å	14.260(4)	14.417(3)	14.454(2)	17.522(2)
α , deg	84.95(2)	95.205(5)	95.640(3)	84.498(9)
β , deg	77.65(1)	102.583(4)	102.821(4)	74.313(7)
γ , deg	90.21(2)	90.720(3)	90.174(3)	72.402(7)
<i>V</i> , Å ³	2502(1)	2527.3(8)	2549.5(6)	2498.6(5)
<i>Z</i>	2	2	2	2
$2\theta_{\max}$	55.0	55.0	55.0	55.0
<i>F</i> (000)	1185.0	1201.0	1222.0	1226.0
<i>D</i> _{calcd} , g/cm ³	1.531	1.534	1.545	1.582
abs coeff, cm ⁻¹	8.30	8.23	8.17	8.35
no. of reflns collcd	17 078	20 591	21 411	21 570
no. of indpt reflns	10 801 (<i>I</i> ≥ 0σ(<i>I</i>))	10 852 (<i>I</i> ≥ 0σ(<i>I</i>))	10 956 (<i>I</i> = 0σ(<i>I</i>))	10 627 (<i>I</i> = 0σ(<i>I</i>))
no. of refined params	654	652	670	667
goodness of fit indication	1.42	1.83	1.73	1.75
largest peak/hole, e Å ⁻³	1.16/-0.72	1.51/-1.25	1.43/-1.14	1.35/-1.57
<i>R</i> ^a	0.103	0.090	0.087	0.060
<i>R</i> _w ^b	0.097	0.122	0.119	0.088
<i>R</i> ₁ ^c	0.071	0.078	0.074	0.054

^a *R* = $\sum[|F_o| - |F_c|]/\sum|F_o|$ (*I* = 0.0σ(*I*)). ^b *R*_w = $[\sum w(|F_o| - |F_c|)^2/\sum w|F_o|^2]^{1/2}$; *w* = $1/[\sigma^2(F_o) + p^2|F_o|^2/4]$ (*p* = 0.065 for **1**·C₂H₅OH; *p* = 0.092 for **2**·C₂H₅OH; *p* = 0.098 for **3**·C₂H₅OH; *p* = 0.074 for **4**). ^c *R*₁ = $\sum[|F_o| - |F_c|]/\sum|F_o|$ (*I* = 2.0σ(*I*)).

4.4; Ni, 5.0. IR (Nujol, cm⁻¹): 1606 (C=C, aromatic), 1097 (ClO₄⁻), 623 (ClO₄⁻).

[Cr₂(μ -OH)₂(phen)₄](ClO₄)₄·3H₂O (**5**)¹⁹ and [Ni₂(μ -OH)₂(tpa)₂](ClO₄)₂ (**6**).²⁰ These were synthesized according to literature methods.

Measurements. Electronic spectra were obtained on a Hitachi U-3400 spectrophotometer. Infrared spectra were obtained by the Nujol-mull method with a Horiba FT-200 spectrophotometer. ¹H NMR spectra were measured with a JEOL JNM-LA400 spectrometer using tetramethylsilane (TMS) as the internal standard. Magnetic susceptibilities were measured by a SQUID susceptometer, Quantum Design MPMS model, which was calibrated with Hg[Co(NCS)₄]. Diamagnetic correction was made using Pascal's constants.²¹ Quantitative analyses of nickel and chromium were carried out by a Hitachi Z-6100 polarized Zeeman atomic absorption spectrophotometer.

X-ray Crystallography. General Procedures. Data collection were carried out at -150 °C on a Rigaku/MSU Mercury diffractometer with graphite-monochromated Mo K α radiation (λ = 0.710 70 Å). Crystal-to-detector distances were 35.2 mm, and detector swing angles were 10.0° for all the measurements. Exposure rates were 40.0, 30.0, 30.0, and 10.0 s/deg for **1**·C₂H₅OH, **2**·C₂H₅OH, **3**·C₂H₅OH, and **4** (vide infra), respectively. Intensity measurements were done using ω scans from -80.0 to 100.0° in 0.50° steps at χ = 45.0° and ϕ = 0.0° and at χ = 45.0° and ϕ = 90.0°. A total of 720 oscillation images were collected. Intensity data were collected to a maximum 2θ value of 55.0°. The data were corrected for Lorentz and polarization effects. Empirical absorption corrections were applied. Crystallographic data are summarized in Table 1.

The structures were solved by a direct method (SIR92)²² and expanded using the Fourier technique.²³ The structures were refined by the full-matrix least-squares method by using the teXsan²⁴ crystallographic software package (Molecular Structure Corp.). Non-hydrogen atoms were refined with anisotropic displacement parameters. Hydrogen atoms were positioned at calculated positions. They were included, but not refined, in the final least-squares cycles. The maximum peaks on final difference Fourier maps were observed close to the solvated ethanol or water molecules. Tables of final atomic coordinates, thermal parameters, and full bond distances and angles are given in the Supporting Information.

[(phen)₂Cr(μ -OH)₂Ni(tpa)](ClO₄)₃·C₂H₅OH·0.75H₂O (1**·C₂H₅OH).** Single crystals suitable for X-ray crystallography were obtained as follows. **1** (50 mg) was dissolved in acetonitrile (4.0 cm³), to which ethanol (16.0 cm³) was added, and the mixture was allowed to stand for several days. Brown needle crystals suitable for X-ray crystallography were obtained. Anal. Calcd for C₄₄H₄₅N₈O_{15.5}Cl₃CrNi: C, 45.29; H, 3.89; N, 9.60. Found: C, 45.20; H, 4.08; N, 9.67.

A single crystal with approximate dimensions of 0.25 × 0.20 × 0.05 mm was mounted on the tip of a glass rod. The asymmetric unit consists of one bis(μ -hydroxo)chromium(III)nickel(II) cation, three perchlorates, two ethanol molecules with a half occupation, and 0.75 water molecules. The final *R* and *R*_w values were 0.103 and 0.097, respectively. The maximum peak on a final difference Fourier map was 1.16 e Å⁻³.

[(phen)₂Cr(μ -OH)₂Ni(Me-tpa)](ClO₄)₃·C₂H₅OH·0.75H₂O (2**·C₂H₅OH).** Green plate crystals suitable for X-ray crystallography

(19) Josephsen, J.; Schäffer, C. E. *Acta Chem. Scand.* **1970**, *24*, 2929–2942.

(20) Ito, M.; Sakai, K.; Tsubomura, T.; Takita, Y. *Bull. Chem. Soc. Jpn.* **1999**, *72*, 239–247.

(21) Mabbs, F. E.; Marchin, D. J. *Magnetism and Transition Metal Complexes*; Chapman and Hall: London, 1975; p 5.

(22) Altomare, A.; Burla, M. C.; Camalli, M.; Cascarano, M.; Giacovazzo, C.; Guagliardi, A.; Polidori, G. *J. Appl. Crystallogr.* **1994**, *27*, 435.

(23) Beurskens, P. T.; Admiraal, G.; Beurskens, G.; Bosman, W. P.; de Gelder, R.; Israel, R.; Smits, J. M. M. *The DIRDIF-94 program system*; Technical Report of the Crystallography Laboratory, University of Nijmegen: Nijmegen, The Netherlands, 1994.

(24) *teXsan: Crystal Structure Analysis Package*; Molecular Structure Corp: The Woodlands, TX, 1985, 1992.

were obtained by recrystallization in a manner similar to that of **1**. Anal. Calcd for $C_{45}H_{45.5}N_8O_{15.75}Cl_3CrNi$: C, 46.30; H, 3.93; N, 9.60. Found: C, 46.21; H, 4.03; N, 9.47.

A single crystal with approximate dimensions of $0.25 \times 0.20 \times 0.08$ mm was mounted on the tip of a glass rod. There are one bis(μ -hydroxo)chromium(III)nickel(II) cation, three perchlorates, an ethanol molecule, and 0.75 water molecules in the asymmetric unit. Oxygen atoms of a perchlorate and water molecules were disordered. The final R and R_w values were 0.090 and 0.122, respectively. The maximum peak on a final difference Fourier map was $1.51 \text{ e } \text{\AA}^{-3}$.

[(phen)₂Cr(μ -OH)₂Ni(Me₂-tpa)](ClO₄)₃·C₂H₅OH·H₂O (3·C₂H₅-OH). Recrystallization of **3** in a manner similar to that of **1** gave green crystals suitable for X-ray crystallography. Anal. Calcd for $C_{46}H_{48}N_8O_{16}Cl_3CrNi$: C, 46.59; H, 4.08; N, 9.45. Found: C, 46.35; H, 4.13; N, 9.65.

A single crystal with approximate dimensions of $0.30 \times 0.20 \times 0.08$ mm was mounted on the tip of a glass rod. The asymmetric unit consists of one bis(μ -hydroxo)chromium(III)nickel(II) cation, three perchlorates, an ethanol, and a water molecule. Oxygen atoms of two perchlorates were disordered, and they were refined with isotropic displacement parameters. The final R and R_w values were 0.087 and 0.119, respectively. The maximum peak on a final difference Fourier map was $1.43 \text{ e } \text{\AA}^{-3}$.

[(phen)₂Cr(μ -OH)₂Ni(Me₃-tpa)](ClO₄)₃·3H₂O (4). A single crystal with approximate dimensions of $0.40 \times 0.40 \times 0.30$ mm was mounted on the tip of a glass rod. There are one bis(μ -hydroxo)chromium(III)nickel(II) cation, three perchlorates, and three water molecules in the asymmetric unit. The final R and R_w values were 0.060 and 0.088, respectively. The maximum peak on a final difference Fourier map was $1.35 \text{ e } \text{\AA}^{-3}$.

Results and Discussion

Heterodimetal chromium(III)–nickel(II) complexes, $[(phen)_2Cr(\mu-OH)_2Ni(Me_n-tpa)]^{3+}$ ($n = 0-3$), were selectively obtained in high yields (72–88%) by simple mixing of a methanol solution of $[Cr(OH)_2(phen)_2]^+$ generated by the reaction of $[Cr(OH)_2(phen)_2]^{3+}$ with a methanol solution containing $Ni(ClO_4)_2 \cdot 6H_2O$ and Me_n-tpa . To our knowledge, these are the first discrete chromium(III)–nickel(II) dimers with a $Cr(\mu-OH)_2Ni$ core.

X-ray Structure Descriptions of 1·C₂H₅OH, 2·C₂H₅OH, 3·C₂H₅OH, and 4. The structures of the heterodimetal cations of **1**·C₂H₅OH and **4** are shown in Figure 1 (those of **2**·C₂H₅OH and **3**·C₂H₅OH are given in Figures S1 and S2 in the Supporting Information). Selected bond distances and angles of all the complexes are given in Table 2. The structures of **1**·C₂H₅OH, **2**·C₂H₅OH, **3**·C₂H₅OH, and **4** resemble one another in having an edge-shared bioctahedral structure with a $Cr(\mu-OH)_2Ni$ unit. Chromium and nickel ions are coordinated by two phen's and Me_n-tpa , respectively, to complete a distorted octahedral coordination sphere. Crystal structures of **2**·C₂H₅OH and **3**·C₂H₅OH revealed that the 6-methylpyridyl groups in the nickel centers coordinate in the apical position(s). It is interesting to compare the structures of the chromium and nickel centers of the heterodimetal complexes with those in the homodimetal complexes, $[Cr_2(\mu-OH)_2(phen)_4]^{4+}$ (**5**),²⁵ $[Ni_2(\mu-OH)_2(tpa)_2]^{2+}$ (**6**),²⁰ and $[Ni_2-$

Table 2. Selected Bond Distances and Angles of **1**·C₂H₅OH, **2**·C₂H₅OH, **3**·C₂H₅OH, and **4**

	1 ·C ₂ H ₅ OH	2 ·C ₂ H ₅ OH	3 ·C ₂ H ₅ OH	4
Bond Lengths (Å)				
Cr–O1	1.914(3)	1.916(3)	1.918(3)	1.927(2)
Cr–O2	1.906(3)	1.908(3)	1.903(3)	1.902(2)
Cr–N1	2.072(3)	2.078(3)	2.081(3)	2.069(2)
Cr–N2	2.101(4)	2.100(3)	2.105(3)	2.088(2)
Cr–N3	2.096(4)	2.100(3)	2.099(3)	2.100(2)
Cr–N4	2.054(4)	2.061(3)	2.066(3)	2.071(2)
Ni–O1	2.034(3)	2.046(3)	2.051(3)	2.056(2)
Ni–O2	2.089(3)	2.101(3)	2.118(3)	2.095(2)
Ni–N5	2.087(4)	2.079(3)	2.076(3)	2.062(2)
Ni–N6	2.046(4)	2.068(4)	2.097(4)	2.149(2)
Ni–N7	2.091(4)	2.118(4)	2.152(3)	2.184(2)
Ni–N8	2.077(4)	2.112(4)	2.142(3)	2.247(2)
Cr···Ni	3.062(1)	3.093(1)	3.115(1)	3.140(1)
Bond Angles (deg)				
O1–Cr–O2	82.4(1)	81.5(1)	81.0(1)	79.51(8)
O1–Ni–O2	75.3(1)	74.0(1)	73.1(1)	72.30(7)
Cr–O1–Ni	101.7(1)	102.6(1)	103.4(1)	104.01(8)
Cr–O2–Ni	99.9(1)	100.9(1)	101.4(1)	103.43(9)
O1–Ni–N6	104.3(1)	106.6(1)	109.8(1)	112.06(9)
O1–Ni–N5	170.4(1)	168.9(1)	166.3(1)	163.25(9)
O2–Ni–N5	97.1(1)	95.7(1)	93.6(1)	91.02(8)

$(\mu-OH)_2(Me_3-tpa)_2]^{2+}$ (**7**)¹⁵ (Table 3). The average Ni–O bond distances in **1**·C₂H₅OH–**4** are in the range of 2.062–2.085 Å, which are substantially longer than those of **6** (2.012 Å)²⁰ and **7** (2.018 Å).¹⁵ On the other hand, the average Cr–O bond distances in **1**·C₂H₅OH–**4** (1.910–1.915 Å) are shorter than that of **5** (1.927 Å).²⁵ This implies that the bridging hydroxide coordinates more strongly to the chromium(III) ion in **1**·C₂H₅OH–**4** compared to that in **5** and the stronger Cr–O bonds in **1**·C₂H₅OH–**4** seem to weaken the Ni–O bonds. The Cr–N(axial) bond distances of **1**·C₂H₅OH–**4** (2.063–2.074 Å) are comparable to those of **5** (2.055 Å), whereas the Cr–N(equatorial) bond distances (2.094–2.102 Å) are significantly longer than those of **5** (2.051 Å). This is also due to the stronger Cr–O bonds in **1**·C₂H₅OH–**4** compared with those in **5**, which may weaken the Cr–N(equatorial) bonds in the trans positions.

The most striking structural feature in **1**·C₂H₅OH–**4** is a systematic structural change at the nickel center depending on the number of the 6-methylpyridyl groups on the Me_n-tpa ligand, which has significant influence on the electronic spectra and the magnetism of the complexes (vide infra). The average Ni–N bond distances of the axial bonds of **1**·C₂H₅OH–**4** increase from 2.084 to 2.216 Å (Table 3). Such a substantial elongation of the Ni–N bonds seems to be mainly due to unfavorable steric interactions between the hydrogen atoms of the 6-methyl group and the bridging hydroxide as found for the complexes with the 6-methylpyridyl group.^{12–15,17} A similar elongation is also observed for the equatorial Ni–N(6-methylpyridyl) bond in **4**. Thus the introduction of the methyl group onto the 6-position of the pyridyl group causes a substantial elongation of the Ni–N(6-methylpyridyl) bonds compared to the Ni–N(pyridyl) bonds. In contrast, the Ni–N(tertiary amine) bonds become shorter as the Ni–N(aromatic) bonds become longer as seen in Table 3. This suggests that the elongation of the Ni–N(aromatic) bonds of such tripodal ligands tends to strengthen the Ni–N(tertiary amine) bonds and make them shorter. A

(25) Veal, J. T.; Hatfield, W. E.; Hodgson, D. J. *Acta Crystallogr.* **1973**, *B29*, 12–20.

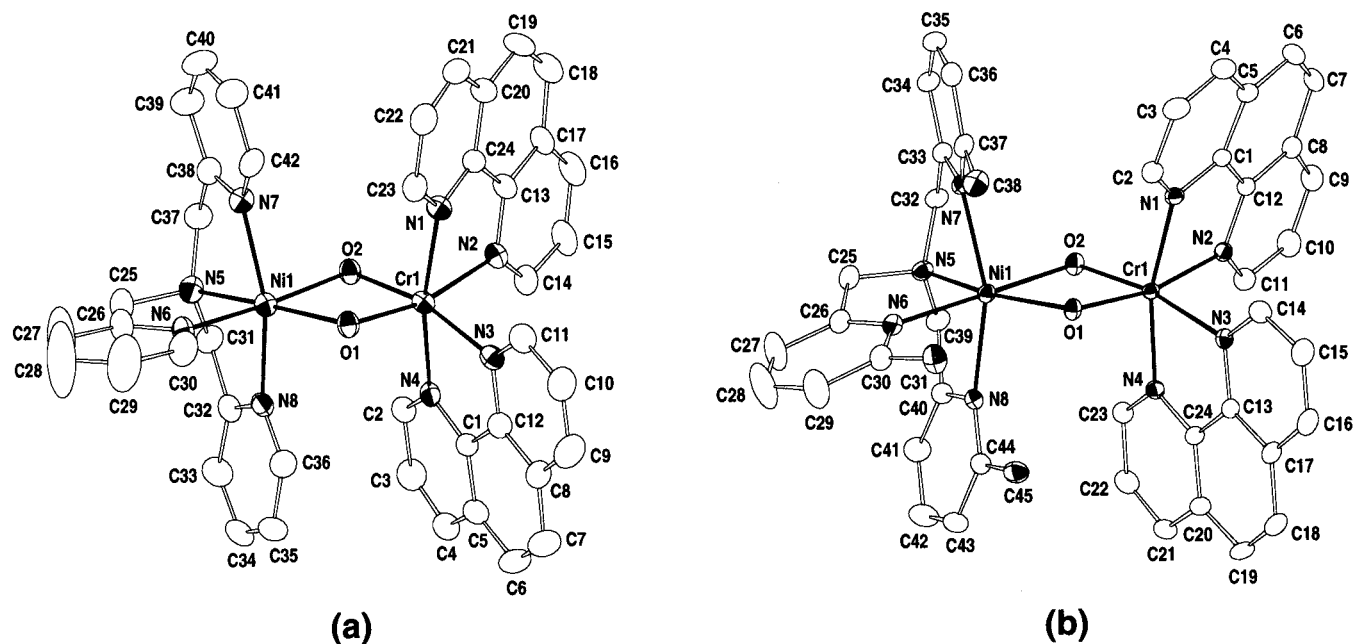


Figure 1. ORTEP views (50% probability) of complex cations of **1**·C₂H₅OH (a) and **4** (b). Hydrogen atoms are omitted for clarity.

Table 3. Structural Comparison of Heterodimetal and Homodimetal Complexes

	1·C ₂ H ₅ OH	2·C ₂ H ₅ OH	3·C ₂ H ₅ OH	4	5 ^a	6 ^b	7 ^c
	Bond Lengths (Å)						
Cr–O _{av}	1.910	1.912	1.911	1.915	1.927		
Cr–N(axial) _{av}	2.063	2.070	2.074	2.070	2.055		
Cr–N(equatorial) _{av}	2.099	2.100	2.102	2.094	2.051		
Ni–O _{av}	2.062	2.074	2.085	2.076		2.012	2.018
Ni–N(axial) _{av}	2.084	< 2.115	< 2.147	< 2.216		2.116	2.246
Ni–N(equatorial) _{av}	2.067	< 2.074	< 2.087	< 2.106		2.102	2.116
{Ni–N(tertiary amine)}	2.087(4)	> 2.079(3)	> 2.076(3)	> 2.062(2)		2.114(5)	2.089(3)
{Ni–N(pyridyl)}	2.046(4)	< 2.068(4)	< 2.097(4)	< 2.149(2)		2.090(5)	2.142(3)
Cr···Ni	3.062(1)	< 3.093(1)	< 3.115(1)	< 3.140(1)	3.008(3)		3.095
	Bond Angles (deg)						
Cr–O–(Ni _{av} or Cr _{av})	100.8	< 101.8	< 102.4	103.72	102.7		
O–Cr–O	82.4(1)	> 81.5(1)	> 81.0(1)	> 79.51(8)	77.3		
O–Ni–O	75.3(1)	> 74.0(1)	> 73.1(1)	> 72.30(7)		82.1(2)	80.1(1)

^a Reference 25. ^b Reference 20. ^c Reference 15.

remarkable systematic change is also observed in the O1–Ni–N6 angles expanding successively from 104.3(1) to 112.06(9)°, which appears to be attributable to the steric interactions between the hydrogen atoms of the 6-methylpyridyl group(s) in the nickel center and the hydrogen atoms of the bridging hydroxo and/or hydrogen atom of the C2 carbon of phen in the chromium center. The expansion of the O1–Ni–N6 angle causes the shrinking of the O1–Ni–N5 and O2–Ni–N5 angles from 170.4(1) to 163.25(9)° and from 97.1(1) to 91.02(8)°, respectively. Thus successive introduction of three methyl groups onto tpa causes a systematic elongation in the average Ni–N bond distances and the expansion and shrinking of the bond angles around nickel centers.

There are also small but systematic changes in the Cr(μ -OH)₂Ni unit structure, which are the Cr···Ni separations (from 3.062(1) to 3.140(1) Å), the average Cr–O–Ni angles (from 100.8 to 103.72°), the O–Ni–O angles (from 75.3–(1) to 72.30(7)°), and the O–Cr–O angles (from 82.4(1) to 79.51(8)°) as seen in Table 3. Steric interactions between the hydrogen atoms of the 6-methylpyridyl group in the

apical position(s) in the nickel center and the hydrogen atom of the C2 atom of phen in the chromium center also increase the Cr···Ni separation (Figure 1b and Figure S2), leading to the expansion of the Cr–O–Ni angle and the reduction of the O–Ni–O and O–Cr–O angles. Such systematic structural changes, however, have no significant influence on the Ni–O and the Cr–O bond distances as already mentioned. The least-squares planes defined by Cr, O1, O2, N2, and N3, and Ni, O1, O2, N5, and N6 for **1**·C₂H₅OH–**4** are slightly bent each other. Dihedral angles between those planes are 13.5(1), 13.50(9), 13.57(9), and 11.09(6)°, indicating the absence of a systematic change. In contrast to the nickel centers, there is no systematic change in the chromium(III) centers (Table 3).

Electronic Spectra. The electronic spectral data for **1–4** in acetonitrile are listed in Table 4. The spectra of **1** and homodimetal complexes (**5** and **6**) are shown in Figure 2. The spectrum of **5** shows a band at 19 200 cm⁻¹ (ϵ /Cr = 45 mol⁻¹ dm³ cm⁻¹) assignable to the d–d band (⁴A_{2g} → ⁴T_{2g}) of an octahedral chromium(III) ion, and that of **6** displays two d–d bands at 10 400 cm⁻¹ (ϵ /Ni = 16 mol⁻¹ dm³ cm⁻¹)

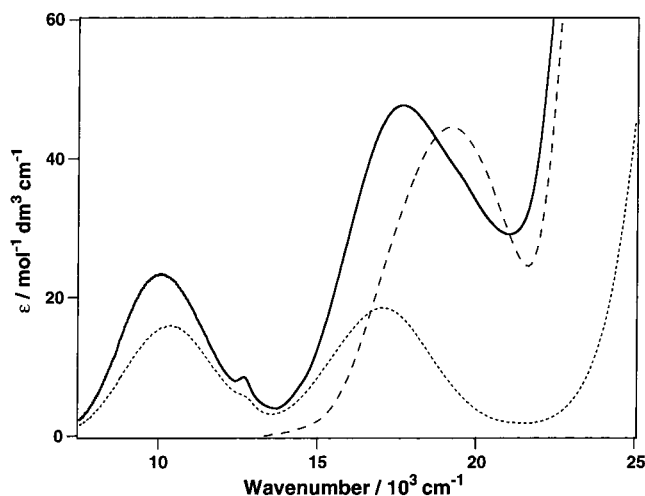


Figure 2. Electronic spectra of **1** (—), **5** (---), and **6** (···) in acetonitrile.

Table 4. Electronic Spectral Data for **1–6** in Acetonitrile

complex	abs band max [$\tilde{\nu}/10^3 \text{ cm}^{-1}$ ($\epsilon/\text{mol}^{-1} \text{ dm}^3 \text{ cm}^{-1}$)]		
1	10.1 (23)	12.7 (9)	17.7 (48)
2	9.7 (23)	12.7 (7)	17.4 (45)
3	9.4 (22)	12.7 (6)	17.4 (44)
4	8.9 (24)	12.8 (9)	17.4 (48)
5	19.2 (45)		
6	10.4 (16)	12.8 sh (6)	17.1 (19)

and $17\,100 \text{ cm}^{-1}$ ($\epsilon/\text{Ni} = 19 \text{ mol}^{-1} \text{ dm}^3 \text{ cm}^{-1}$) attributable to the ${}^3\text{A}_{2g} \rightarrow {}^3\text{T}_{2g}(\text{F})$ and ${}^3\text{A}_{2g} \rightarrow {}^3\text{T}_{1g}(\text{F})$ transitions of an octahedral nickel(II) ion. As can be seen in Figure 2, the spectrum of **1** shows two absorption bands at $10\,100 \text{ cm}^{-1}$ ($\epsilon = 23 \text{ mol}^{-1} \text{ dm}^3 \text{ cm}^{-1}$) and $17\,700 \text{ cm}^{-1}$ ($\epsilon = 48 \text{ mol}^{-1} \text{ dm}^3 \text{ cm}^{-1}$), which are assigned to the ${}^3\text{A}_{2g} \rightarrow {}^3\text{T}_{2g}$ transition of the nickel(II) center and to a superposition of the ${}^4\text{A}_{2g} \rightarrow {}^4\text{T}_{2g}$ transition of the chromium(III) center and the ${}^3\text{A}_{2g} \rightarrow {}^3\text{T}_{1g}(\text{F})$ transition of the nickel center, respectively.

The transition energies of the higher energy bands which are dominated by the d–d band of chromium(III) center are almost the same for all the complexes ($17\,700$ – $17\,400 \text{ cm}^{-1}$ in Table 4), indicating that there is no remarkable change in the ligand field strengths of the chromium(III) centers, which is in line with the crystal structural results discussed above. In contrast, a successive change in the d–d transition energies of the nickel centers is observed from $10\,100$ to 8900 cm^{-1} . As the number of the methyl groups of the ligands increases, the band maximum shifts to a lower energy side, **1** > **2** > **3** > **4**. This can be interpreted in terms of the weakening of the ligand field strengths of $\text{Me}_n\text{-tpa}$ due to the elongation of the Ni–N bonds. A successive shift amounts to $\sim 400 \text{ cm}^{-1}$ per methyl group (Table 4).

Magnetism. Variable-temperature magnetic susceptibilities for powdered samples of **1–4** were measured over the temperature range 4.2 – 300 K . Plots of temperature dependence of the effective magnetic moments ($\mu_{\text{eff}}/\text{Cr–Ni}$) are given in Figure 3. The magnetism was analyzed by the isotropic exchange interaction model including an axial zero field splitting given in eq 1. The magnetic susceptibility data (χ_M) were fitted to eq 2, where $x_D = \exp(-D/3kT)$, $x = \exp(-J/kT)$, the g factors (g_1 , g_2 , and g_3) are $3/5g_{\text{Cr}} + 2/5g_{\text{Ni}}$, $11/15g_{\text{Cr}} + 4/15g_{\text{Ni}}$, and $5/3g_{\text{Cr}} - 2/3g_{\text{Ni}}$, respectively, and

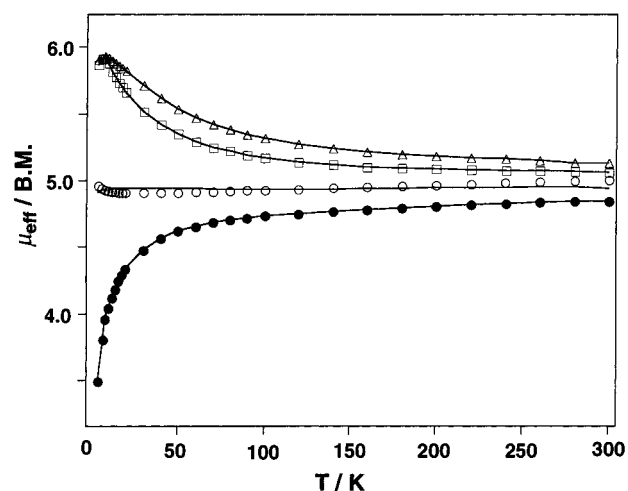


Figure 3. Temperature dependencies of the effective magnetic moments for **1** (●), **2** (○), **3** (□), and **4** (△). The solid lines are the best-fit curves with the parameters given in Table 5. Details are given in the text.

D is the axial zero field splitting parameter for an $S = 5/2$ ground state (in the case of antiferromagnetic interaction, D is set to zero). TIP is a temperature-independent paramagnetism which was fixed at $5 \times 10^{-4} \text{ cgs emu mol}^{-1}$, except for the case of **1** in which the value of TIP was set to zero. The other symbols have their usual meanings. Equation 2 is valid only under the condition $|D| \ll J$. Since octahedral Cr(III) complexes do not have significant spin–orbit coupling, the value of g_{Cr} was set to 2.0. The magnetic parameters estimated are listed in Table 5.

$$\mathbf{H} = \beta(g_{\text{Cr}}\mathbf{S}_{\text{Cr}} + g_{\text{Ni}}\mathbf{S}_{\text{Ni}})H - 2J\mathbf{S}_{\text{Cr}}\cdot\mathbf{S}_{\text{Ni}} + D[S_z^2 - (1/3)S(S+1)]\delta_{S,5/2} \quad (1)$$

$$\chi_M = [N\beta^2/4k(T - \Theta)] \{ [25g_1^2x_D^{10} + 9g_1^2x_D^{-2} + g_1^2x_D^{-8} + 10g_2^2x^5 + g_3^2x^8] / (x_D^{10} + x_D^{-2} + x_D^{-8} + 2x^5 + x^8) \} + \text{TIP} \quad (2)$$

The effective magnetic moment for **1** decreases from $4.87 \mu_B$ at 300 K to $3.49 \mu_B$ at 4.2 K . The least-squares fitting shown as a solid line in Figure 3 gave $g_{\text{Ni}} = 2.05$, $J = -1.35 \text{ cm}^{-1}$, indicating the presence of a very weak antiferromagnetic interaction between chromium(III) and nickel(II) ions. The effective magnetic moment of **2** (4.95 – $4.91 \mu_B$) is almost constant over the temperature range (300 – 4.2 K). The best fit parameters are $g_{\text{Ni}} = 2.09$, $J = 0.00 \text{ cm}^{-1}$. Complex **3** showed an increase of the effective magnetic moment from $5.06 \mu_B$ at 300 K to $5.91 \mu_B$ at 6 K and a slight decrease below 6 K . This suggests that two metal ions are ferromagnetically coupled. In fact, the magnetization experiments of **3** and **4** as a function of the applied field at 4.2 K revealed that the experimental values are fitted to the values estimated by the Brillouin function for an $S = 5/2$ system (see Figure S3 in the Supporting Information), although some deviations from the theoretical values may be due to the contribution arising from some other factors such as antiferromagnetic interaction between dimers and/or zero-field splitting (vide infra). The temperature dependence of the effective magnetic moments was analyzed in

Table 5. Comparison of Magnetic Data for Heterometal Cr(III)–Ni(II) Complexes^a

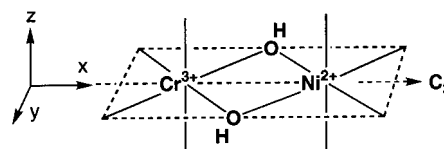
complex	J (cm ⁻¹)	g_{Cr}^b	g_{Ni}	Θ (K)	D (cm ⁻¹)	ref
1	-1.35	2.00	2.05			this work
2	0.00	2.00	2.09			this work
3	+4.07	2.00	2.09		0.051	this work
	+4.10	2.00	2.10	-0.31		
4	+7.58	2.00	2.06		0.065	this work
	+7.38	2.00	2.07	-0.23		
8 (Cr(μ -OH) ₂ Ni)	-2.4					9
9 (Cr(μ -OH)Ni)	-4.2					10
10 (Cr(μ -ox)Ni)	+2.7					1
11 (Cr(μ -ox)Ni)	+3.6					2
12 (Cr(μ -ox)Ni)	+4.6					3
13 (Cr(μ -dto)Ni)	+5.9					4a
14 (Cr(μ -CN)Ni)	+8.4					6

^a Abbreviations of complexes: **8** = [Ni{(OH)₂Cr(bispictn)}₃](ClO₄)₅·6H₂O; **9** = [Ni(H₂O)₄{(OH)Cr(picO)₂(OH)}₂](S₂O₆)₂·H₂O; **10** = [Cr{(ox)Ni(Me₆-[14]ane-N₄)₃}(ClO₄)₃]; **11** = {NBu₄[NiCr(ox)₃]}_x; **12** = [Cr(salen)(ox)Ni(taea)](BPh₄)·MeOH; **13** = [Cr{(dto)Ni(Me₆-[14]ane-N₄)₃}(ClO₄)₃]; **14** = [Cr{(CN)Ni(tetren)}₆](ClO₄)₉. ^b g_{Cr} is fixed to 2.00.

two ways: (1) $\Theta = 0$, $D = \text{variable}$; (2) $\Theta = \text{variable}$, $D = 0$. The parameters obtained by the former are $g_{Ni} = 2.09$, $J = +4.07 \text{ cm}^{-1}$, and $D = 0.051 \text{ cm}^{-1}$, and those by the latter are $g_{Ni} = 2.10$, $J = +4.10 \text{ cm}^{-1}$, and $\Theta = -0.31 \text{ K}$. Both gave almost the same convergence factors, suggesting that the slight decrease of the magnetic moments below 10 K is due to the contribution of the zero field splitting of an $S = 5/2$ ground state and/or a weak interdimer antiferromagnetic interaction. The effective magnetic moment of **4** also increases from $5.13 \mu_B$ at 300 K to $5.93 \mu_B$ at 8 K and slightly decreases below 8 K, implying the presence of a ferromagnetic interaction between chromium(III) and nickel(II) ions. The analyses by the above two methods gave the parameters $g_{Ni} = 2.06$, $J = +7.58 \text{ cm}^{-1}$, and $D = 0.065 \text{ cm}^{-1}$ and $g_{Ni} = 2.07$, $J = +7.38 \text{ cm}^{-1}$, and $\Theta = -0.23 \text{ K}$, respectively. The results also suggest the presence of zero field splitting of an $S = 5/2$ ground state and/or a weak interdimer antiferromagnetic interaction.

A striking feature of the magnetism of these complexes is a systematic change from a very weak antiferromagnetic interaction to ferromagnetic interaction between chromium(III) and nickel(II) ions depending on the number of the 6-methylpyridyl groups; J values of **1–4** vary from -1.4 through 0.0 cm^{-1} and $+4.1$ to $+7.4 \text{ cm}^{-1}$. Such a systematic change in the exchange integrals may allow us to study the magneto–structural relationship in the heterodimetal chromium(III)–nickel(II) ions. As already mentioned, heterodimetal chromium(III)–nickel(II) complexes having hydroxo bridges exhibit a weak antiferromagnetic interaction.⁹ Complexes **3** and **4** are the first ferromagnetically coupled complexes with hydroxo bridges.

Theoretical treatments of the magnetic interactions between metal ions have been based on the interactions between the magnetic orbitals.^{26,27} The exchange integral J_{Cr-Ni} between chromium(III) and nickel(II) ions may be expressed by a sum of J_{ij} 's which represent the pairwise interactions between the magnetic orbitals.²⁷ The three unpaired electrons of chromium(III) ion in an octahedral environment occupy the three t_{2g} type magnetic orbitals, $d_{x^2-y^2}$, d_{xz} , and d_{yz} , and

Chart 1

the two unpaired electrons of nickel(II) ions in an octahedral environment are in the e_g type magnetic orbitals, d_{xy} and d_{z^2} (Chart 1). Assuming that the symmetry of the Cr(μ -OH)₂Ni unit in the present complexes is C_{2v} , the t_{2g} type magnetic orbitals are transformed as $a_1(d_{x^2-y^2})_{Cr}$, $b_2(d_{xz})_{Cr}$, and $a_2(d_{yz})_{Cr}$ and the e_g type magnetic orbitals as $a_1(d_{z^2})_{Ni}$ and $b_1(d_{xy})_{Ni}$ shown in Chart 1. Then J_{Cr-Ni} is expressed by the following:

$$J_{Cr-Ni} = \{J[a_1(d_{x^2-y^2})_{Cr}a_1(d_{z^2})_{Ni}] + J[b_2(d_{xz})_{Cr}a_1(d_{z^2})_{Ni}] + J[a_2(d_{yz})_{Cr}a_1(d_{z^2})_{Ni}] + J[a_1(d_{x^2-y^2})_{Cr}b_1(d_{xy})_{Ni}] + J[b_2(d_{xz})_{Cr}b_1(d_{xy})_{Ni}] + J[a_2(d_{yz})_{Cr}b_1(d_{xy})_{Ni}]\} / 6 \quad (3)$$

In eq 3, all the J_{ij} 's are positive due to the orbital orthogonality of the magnetic orbitals which contribute to ferromagnetic interactions²⁷ except for $J[a_1(d_{x^2-y^2})_{Cr}a_1(d_{z^2})_{Ni}]$, which is negative to lead to an antiferromagnetic interaction. The magnetic properties of the present complexes depend on a delicate balance between relative magnitudes of $J[a_1(d_{x^2-y^2})_{Cr}a_1(d_{z^2})_{Ni}]$ and $\{J[b_2(d_{xz})_{Cr}a_1(d_{z^2})_{Ni}] + J[a_2(d_{yz})_{Cr}a_1(d_{z^2})_{Ni}] + J[a_1(d_{x^2-y^2})_{Cr}b_1(d_{xy})_{Ni}] + J[b_2(d_{xz})_{Cr}b_1(d_{xy})_{Ni}] + J[a_2(d_{yz})_{Cr}b_1(d_{xy})_{Ni}]\}$.

Since J_{ij} is proportional to a mixing between two magnetic orbitals, the observed change in the magnetic interactions of the present complexes may be attributable to a systematic change in the mixing between the $a_1(d_{x^2-y^2})_{Cr}$ and $a_1(d_{z^2})_{Ni}$ orbitals depending on the nature of the Ni ligand. The change from antiferromagnetic interaction to ferromagnetic interaction implies a decrease of the orbital mixing because of the elongation of the average Ni–N bond distances, which would be expected to cause the weakening of the electron donor ability of the nitrogen donors and the lowering of the $a_1(d_{z^2})_{Ni}$ magnetic orbitals. The decrease of the mixing between the $a_1(d_{x^2-y^2})_{Cr}$ and $a_1(d_{z^2})_{Ni}$ orbitals by the lowering of the $a_1(d_{z^2})_{Ni}$ magnetic orbitals may be due to an increase of the energy gap between $a_1(d_{x^2-y^2})_{Cr}$ and $a_1(d_{z^2})_{Ni}$ orbitals; this implies that the energies of $a_1(d_{x^2-y^2})_{Cr}$ orbitals are higher

(26) Hay, P. J.; Thibeault, J. C.; Hoffmann, R. *J. Am. Chem. Soc.* **1975**, *97*, 4884–4899.

(27) Kahn, O. *Struct. Bonding* **1987**, *68*, 89–167.

than those of $a_1(d_{z^2})_{\text{Ni}}$ orbitals. Thus, the magnetic properties of a series of the present complexes can be phenomenologically understood by the energy change of the magnetic orbitals in the nickel centers. This study clearly shows that the magnetic interaction can be modulated by controlling the magnetic orbital energies of the metal ions.

Another possible explanation for the observed systematic change in magnetic behavior of the complexes is to consider the configuration interaction (CI) between the ground state and the charge transfer (CT) excited states arising from the charge transfer from the $p\sigma$ orbitals of the bridging hydroxides to the d_{xy} orbital in the nickel center. Solomon et al. have explained the strong antiferromagnetic interaction between two copper(II) ions in oxyhemocyanin in terms of the valence bond configuration interaction (VBCI) between the singlet ground state and the singlet CT excited state, the latter being significantly stabilized by large and direct overlap between a singly occupied π_{σ}^* orbital of the bridging peroxide and a singly occupied d_{xy} orbital on half of the dimer.²⁸ For the present complexes, it is reasonable to take account of only the CT excited states of the nickel center, since the contribution from the CT excited state arising from the chromium center probably remains constant within this series of complexes because of no significant structural change in the chromium center. In the CT excited state arising from the charge transfer from the $p\sigma$ orbitals of the bridging hydroxides to the d_{xy} orbital in the nickel center, the singly occupied $d_{x^2-y^2}_{\text{Cr}}$, d_{xz}_{Cr} , d_{yz}_{Cr} , $d_{z^2}_{\text{Ni}}$, and oxygen $p\sigma$ orbitals are all orthogonal to each other to stabilize the sextet state. CI with this excited CT state with the sextet state can cause the stabilization of the ground state with the sextet state ($S = 5/2$). There is a possibility that the lowering of the d_{xy} orbital energy of the nickel center stabilizes the excited CT state with an $S = 5/2$ spin state, leading to the increase of the CI interaction. However, CI is only effective when the energy gap between the ground state and the excited state is small. Since the energy gap between the ground state and

the excited state in the present complexes is not currently known, further study is needed to evaluate the above CI effect.

Conclusion. A series of new heterodinuclear bis(μ -hydroxo)chromium(III)-nickel(II) complexes were prepared, $[(\text{phen})_2\text{Cr}(\mu\text{-OH})_2\text{Ni}(\text{Me}_n\text{-tpa})]\text{X}_3$. Successive elongation of the Ni–N bond distances was observed according to the sequence $\mathbf{1} < \mathbf{2} < \mathbf{3} < \mathbf{4}$, which is due to the steric interaction of the 6-methylpyridyl group(s) with the bridging hydroxide. Such elongation of the Ni–N bond distances causes a systematic lowering of the d–d transition energies of the nickel(II) centers, which is due to weakening of the electron donor ability of the nitrogens in the nickel centers. A systematic change in the magnetic interactions from antiferromagnetic to ferromagnetic between the chromium(III) and nickel(II) centers was also found as the number of the 6-methylpyridyl groups increases. This is attributable to lowering of the d-orbital energies on the nickel centers; as a result, the mixing of $a_1(d_{x^2-y^2})_{\text{Cr}}$ and $a_1(d_{z^2})_{\text{Ni}}$ orbitals decreases according to the sequence $\mathbf{1} > \mathbf{2} > \mathbf{3} > \mathbf{4}$, which leads to a decrease of the antiferromagnetic contribution. Thus, these results show that the magnetic interaction can be controlled by the d-orbital energies of the metal ions by modifying the coordination environments. Although molecular magnets composed of Cr(III)–Ni(II) units reported thus far have oxalate or cyanide bridges, a unit containing hydroxide bridges is also a possible candidate as a building block for construction of molecular-based ferromagnets.

Acknowledgment. This work is supported by Grants-in-Aid for Scientific Research from the Ministry of Education, Science, and Culture, Japan (M.S.).

Supporting Information Available: Figures S1 and S2, displaying Ortep drawings of $\mathbf{2}\cdot\text{C}_2\text{H}_5\text{OH}$ and $\mathbf{3}\cdot\text{C}_2\text{H}_5\text{OH}$, Figure S3, showing the magnetization M versus magnetic field H plots of $\mathbf{3}$ and $\mathbf{4}$, and four X-ray crystallographic files, in CIF format. This material is available free of charge via the Internet at <http://pubs.acs.org>.

(28) Tuzek F.; Solomon, E. I. *J. Am. Chem. Soc.* **1994**, *116*, 6916–6924.